


LETTER TO THE EDITOR

Open Access



Differential impact of BRAFV600E isoforms on tumorigenesis in a zebrafish model of melanoma

Raffaella De Paolo^{1,2}, Samanta Sarti^{1,2,3}, Sara Bernardi^{1,2,4}, Francesco Cucco¹, Andrea Tavosanis^{1,2,5}, Letizia Pitto¹ and Laura Poliseni^{1,2*} 

Abstract

BRAFV600E comes as two main splicing variants. The well-studied ref isoform and the recently discovered X1 isoform are co-expressed in cancer cells and differ in terms of 3'UTR length and sequence, as well as C-term protein sequence. Here, we use a melanoma model in zebrafish to study the role played by each isoform in larval pigmentation, nevi formation, and their progression into melanoma tumours. We show that both BRAFV600E-ref and BRAFV600E-X1 proteins promote larval pigmentation and nevi formation, while melanoma-free survival curves performed in adult fish indicate that BRAFV600E-ref protein is a much stronger melanoma driver than BRAFV600E-X1 protein. Crucially, we also show that the presence of the 3'UTR suppresses the effect of ref protein. Our data highlight the necessity to undertake a systematic study of BRAFV600E isoforms, in order to uncover the full spectrum of their kinase-(in)dependent and coding-(in)dependent functions, hence to develop more informed strategies for therapeutic targeting.

Keywords Zebrafish, Melanoma modeling, BRAFV600E-ref, BRAFV600E-X1, 3'UTR

Dear Editor,

Melanoma originates from melanocytes and is responsible for the highest mortality among skin cancers. As a result, significant research has been dedicated to its study, and zebrafish models recapitulating the most common genetic alterations have offered several notable contributions to this field [1].

A specific characteristic of melanoma is the recurrent overactivation of the ERK pathway, most often because of the BRAFV600E mutation, which is now routinely targeted by specific inhibitors approved for use by the FDA [2]. The *BRAF* gene is characterised by several splicing variants, and while some of them associated with drug resistance have been well investigated, comparatively little is known about their physiological regulation. Different protein isoforms may exhibit different biological properties, including catalytic capacity, subcellular localization, and protein–protein interaction. Similarly, distinct mRNA isoforms may gain unique binding sites for miRNAs and RNA-binding proteins. In short, investigating the landscape of BRAF isoforms may reveal kinase- and coding-(in)dependent functions that directly or indirectly affect melanoma onset, progression or escape from antineoplastic treatments.

We recently reported that irrespectively of its mutational status human *BRAF* is expressed as a mix of *ref*,

*Correspondence:

Laura Poliseni

laura.poliseni@cnr.it; l.poliseni@ispro.toscana.it

¹ Institute of Clinical Physiology, CNR, Pisa, Italy

² Oncogenomics Unit, Core Research Laboratory (CRL), ISPRO, Via Moruzzi 1, 56124 Pisa, Italy

³ Present Address: Department of Radiation Oncology, Columbia University Irving Medical Center, New York, USA

⁴ Present Address: Department of Molecular Medicine and Neurobiology, IRCCS Fondazione Stella Maris, Pisa, Italy

⁵ Present Address: San Raffaele Telethon Institute for Gene Therapy, IRCCS San Raffaele Scientific Institute, Milan, Italy



© The Author(s) 2023. **Open Access** This article is licensed under a Creative Commons Attribution 4.0 International License, which permits use, sharing, adaptation, distribution and reproduction in any medium or format, as long as you give appropriate credit to the original author(s) and the source, provide a link to the Creative Commons licence, and indicate if changes were made. The images or other third party material in this article are included in the article's Creative Commons licence, unless indicated otherwise in a credit line to the material. If material is not included in the article's Creative Commons licence and your intended use is not permitted by statutory regulation or exceeds the permitted use, you will need to obtain permission directly from the copyright holder. To view a copy of this licence, visit <http://creativecommons.org/licenses/by/4.0/>. The Creative Commons Public Domain Dedication waiver (<http://creativecommons.org/publicdomain/zero/1.0/>) applies to the data made available in this article, unless otherwise stated in a credit line to the data.

X1 and *X2* splicing variants. The *reference* (*ref*) isoform is composed of 18 exons. Exon 18 contains the STOP codon and a short 3'UTR (~100nt). The *X1* isoform is composed of a shorter version of exon 18, which is spliced with a downstream exon 19. This last exon contains the STOP codon and a very long 3'UTR (~7000nt). The *X2* isoform lacks exon 18, with exon 17 directly spliced with exon 19. Also in this case, exon 19 contains the STOP codon, through a different frame, and the very long 3'UTR [3] (see also Additional file 1 : Fig. S1). These isoforms are always co-expressed in cancer cells, with *X1* much more expressed than *ref* and *X2* [3]. Interestingly, *ref* and *X1* 3'UTRs are subjected to post-transcriptional regulation by distinct groups of microRNAs and RBPs. They positively or negatively affect mRNA stability or translation, and, consequently, contribute to fine tune the output of MAPK signaling pathway [4–6]. In terms of proteins, *ref* and *X1* differ at the C-terminal domain (*ref*: –GYGAFPVH vs. *X1*: –GYGEFAAFK), are both endowed with kinase activity, and together account for the known oncogenic features displayed by BRAFV600E in melanoma cells [3, 7] (see also Additional file 1 : Fig. S1). Conversely, *X2* protein is quite unstable and rapidly undergoes proteasome-dependent degradation, due to the presence of K₇₃₉ residue in its C-terminal domain [3].

Here, we use a p53-mutated tumour-prone zebrafish line to compare the BRAFV600E-*ref* isoform with the BRAFV600E-*X1* isoform. We found that BRAFV600E-*ref* protein is a much stronger melanoma driver than BRAFV600E-*X1* protein, but this difference is abolished in presence of the 3'UTR.

Currently, five annotated protein sequences are documented for BRAF and two of them are included in the consensus coding sequence database (CCDS): #220 and #204. Comparing the most updated annotation with our own previous studies [3], we conclude that the *ref* isoform corresponds to #220 and the *X1* isoform corresponds to #204, while *X2* is not currently annotated in the CCDS. Current mRNA sequences are: *NM_004333.6* and *ENST00000646891.2* for *BRAF-ref*, *NM_001354609.2* and *ENST00000496384.7* for *BRAF-X1*, and *NM_001378468.1* for *BRAF-X2*.

To the best of our knowledge, all in vivo cancer models available so far make use of BRAFV600E-*ref* cds [1]. In particular, the expression of Myc-tagged BRAFV600E oncogene in the melanocytic lineage of zebrafish leads to the formation of nevi that progress to melanoma in case of p53 deficiency (*Tg(mitfa:BRAFV600E-Myc);p53(lf)* line [8]). Building up on this, we have developed a model system that allows to compare BRAFV600E-*ref* versus *X1* cds isoforms, as well as to investigate the contribution of the respective 3'UTRs. Specifically, we generated plasmids expressing *ref* or *X1* cds, with or without their 3'UTR (Fig. 1a, see also Additional files 2, 3, 4). As reported in [8], we used *mitfa* promoter to confine the expression of the oncogene in melanocytes. However, we avoided fusing the proteins' C-terminal domain to a tag, as that would compromise our ability to discriminate their different functionalities. As far as 3'UTRs are concerned, their size was chosen based on our previous analysis: 121nt for *ref* and 7163nt for *X1* [3]. Also, we relied on the expression of a cardiac eGFP reporter to screen for plasmid integration. Finally, plasmid cloning

(See figure on next page.)

Fig. 1 Impact of BRAFV600E isoforms on melanomagenesis in zebrafish. **a** Schematic representation of the plasmids that express human BRAFV600E isoforms (*upper*, coding sequence (*ref* cds, *X1* cds, and *X2* cds); *lower*, *ref* cds + 3'UTR, and *X1* cds + 3'UTR) under the control of *mitfa* promoter (*mitfa* prom), and eGFP reporter (green) under the control of cardiac *myl7* promoter (*myl7* prom). Tol2: minimal elements of Tol2 transposon; pA: polyA tail. **b** Pigmentation pattern in larvae at 5dpf. Larvae that were injected at 1-cell stage with *ref* and *X1* cds plasmids show increased number or abnormal appearance of pigmented spots. Left: lateral view; right: lateral zoom view. A 5dpf *Tg(mitfa:mCherry,myl7:eGFP);p53(lf)* larva is shown as negative control (CTR mCh). Scale bars: 500 μ m. **c** Representative examples of a juvenile fish with nevi (*upper*, red arrows), an adult fish with nevi (*middle*, red arrows), and an adult fish with a melanoma tumor (*lower*, red arrow). **d** Percentage of juvenile fish with a nevus. Nevi develop in higher percentage in juveniles injected with *ref* and *X1* cds plasmids. Data are expressed as mean \pm SEM. The number of juvenile fish per experimental condition (*n*) is reported in brackets. Differences were analyzed using Fisher's exact test. **e** Percentage of adult fish with a nevus. Data are expressed as mean \pm SEM. The number of adult fish per experimental condition (*n*) is reported in brackets. Differences were analyzed using Fisher's exact test. No difference reaches statistical significance. **f** Size of nevi in adult fish (3 months of age). Adults injected with *ref* and *X1* cds plasmids show nevi characterized by bigger area. Data are expressed as mean \pm SEM. The number of adult fish per experimental condition (*n*) is reported in brackets. Differences were analyzed using Kruskal–Wallis (Dunn's) test. **g** One-year long melanoma-free survival curves uncover *ref* cds as the most potent melanoma driver compared to *X1* cds, *ref* cds + 3'UTR, and *X1* cds + 3'UTR. The number of adult fish per experimental condition (*n*) is reported in brackets. Differences were analyzed using log-rank (Mantel-Cox) test. **h, i** Macro features of melanoma tumors developed in adults. **h** Tumors localization. **i** Presence of pigmentation. Melanotic tumors develop at higher percentage in fish injected with *ref* cds and *ref* cds + 3'UTR plasmids. The number of adult fish per experimental condition (*n*) is reported in brackets. Differences were analyzed using Fisher's exact test. **j** Representative images of BRAFV600E immunohistochemistry staining (*left*) and Hematoxylin and Eosin staining (H&E, *right*) performed on melanoma tumors in adult fish. Black scale bar: 500 μ m; blue scale bar: 90 μ m. **k** Western blot detection of BRAFV600E (*left, upper*), Mcm7 (*left, lower*) p-Erk 1/2 (*right, upper*) and Erk 2 (*right, lower*) in representative melanoma tumors excised from adult fish. Brain tissue is used as negative control (CTR–). The quantification of Mcm7 and p-Erk/Erk ratio is reported at the bottom of the panels and is expressed as fold change over the negative control. Color coding: yellow: *ref* cds; green: *X1* cds; black: *X2* cds; blue: *ref* cds + 3'UTR; purple: *X1* cds + 3'UTR. Statistically significant differences are indicated with asterisks: **P* < 0.05, ***P* < 0.01, ****P* < 0.001, *****P* < 0.0001

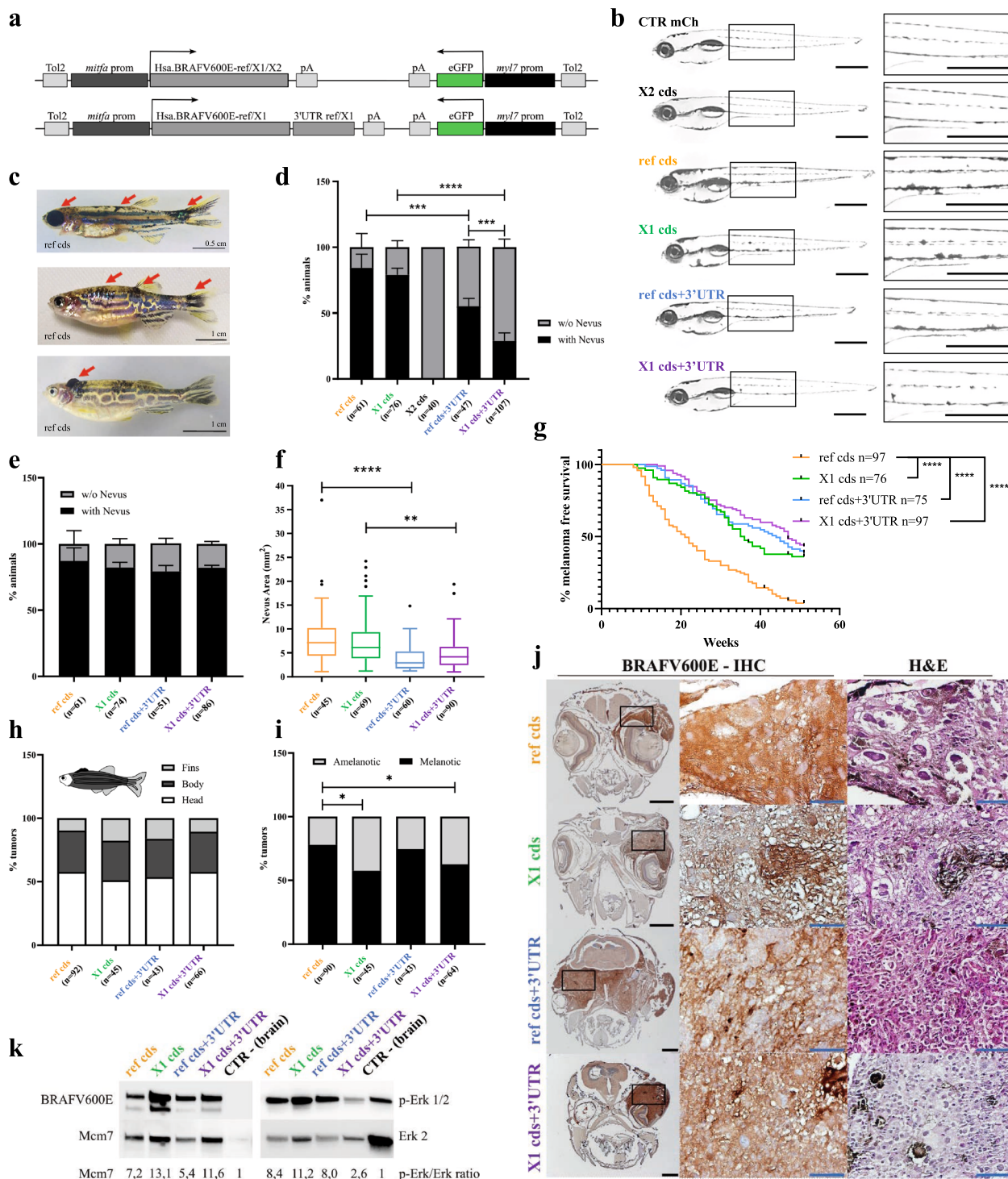


Fig. 1 (See legend on previous page.)

was performed using Tol2kit, so that the DNA portion of the plasmid located between Tol2 elements gets effectively integrated in the zebrafish genome through Tol2-mediated transgenesis.

Plasmids were co-injected with *Transposase* mRNA in 1-cell embryos of the p53-mutant and tumor-prone ZDB-ALT-050428-2 (*p53(lf)*) zebrafish line. At 24 h post fertilization (hpf) we selected successfully injected

embryos based on the presence of a green heart. We also validated the expression of all *BRAFV600E* isoforms, including coding sequence (cds)-only and coding sequence plus 3'UTR (cds+3'UTR) transcripts (Additional file 1 : Fig. S2a, b). mRNA levels were quantified at both 24hpf and 5 days post fertilization (dpf) (Additional file 1 : Fig. S2c, d). Interestingly, we noticed that *X1* cds+3'UTR expression is much higher compared to *ref* cds+3'UTR, in agreement with the data we reported on melanoma samples and cell lines [3].

We thus proceeded to the analysis of the biological consequences of *BRAFV600E* isoform overexpression. The mosaic condition exhibits altered pigmentation starting at the larval stage (5dpf). This phenotype is most apparent for recipients of the *ref* and *X1* cds plasmids, while cds+3'UTR recipients display a milder phenotype (Fig. 1b). Such trend is maintained at the juvenile stage, in terms of percentage of animals showing development of a nevus (Fig. 1c, upper, d and Additional file 1 : Fig. S3a), and upon reaching adulthood, in terms of nevi size (Fig. 1c, middle, e, f and Additional file 1 : Fig. S3b). As expected, the *X2* variant shows no impact at any stage of development. Reflecting the fact that nevi number and size are important clinical prognostic factors in human, we recorded melanoma-free survival curves at the adult stage over a 1-year observation period, focusing on the comparison between *ref* and *X1*. Strikingly, we found that *ref* cds is a much stronger melanoma driver than all the others (Fig. 1c, lower, g and Additional file 1 : Fig. S4), without affecting the development of tumors across the fish body (Fig. 1h), but potentially enhancing the emergence of melanotic tumors (Fig. 1i).

It remains to be elucidated how the few amino acids distinguishing *BRAFV600E-ref* and *-X1* have no impact on nevi development (compare yellow and green in Fig. 1b, d–f), while they have such a dramatic impact on nevi transformation into melanoma (compare yellow and green lines in Fig. 1g). Major alterations in *BRAFV600E* protein levels or ability to activate ERK pathway can be excluded (Fig. 1j, k and Additional file 1 : Fig. S5). However, more detailed analyses in ad hoc experimental settings may reveal subtle differences in substrate preferences. Another possibility is that the different C-terminal domains exert kinase-independent functions, such as interactions with different sets of proteins and activation of different signaling pathways, or are engaged in different regulatory mechanisms.

The milder effect exhibited by the cds+3'UTR plasmids is likely because 3'UTRs are intrinsically devoted to regulation and tuning of gene expression [9]. Nevertheless, several puzzling issues remain: why the short *ref* 3'UTR mildly affects nevi development (compare yellow and blue in Fig. 1b, d–f), but has a dramatic impact on

nevi transformation into melanoma, completely reversing the effect of *ref* cds (compare yellow and blue lines in Fig. 1g)? Conversely, why the long *X1* 3'UTR severely delays nevi development (compare green and purple in Fig. 1b, d–f), in spite of the fact that it ensures higher expression levels to *X1* cds+3'UTR mRNA (compare green and purple bars in Additional file 1 : Fig. S2c, d), and then it has a negligible impact on nevi transformation into melanoma (compare green and purple lines in Fig. 1g)? In general terms, we can speculate that the impact of the *X1* 3'UTR is mild, being the *X1* cds a weak melanoma driver per se, while the *ref* 3'UTR contributes to tame the strong oncogenicity of the *ref* cds. However, the mechanistic details underlying each biological outcome, in each phase of fish life, remain to be uncovered taking advantage of the more homogeneous genetic background provided by stable transgenic lines.

In summary, in this work we show that different cds and 3'UTR sequences of *BRAFV600E* differentially affect tumorigenesis in a zebrafish melanoma model. This experimental data urge to undertake a systematic analysis of *BRAFV600E* isoforms beyond the *ref* kinase, which so far has catalyzed the attention of the melanoma scientific community. Populating the field of kinase- and coding-(in)dependent functions of *BRAFV600E* isoforms can in turn prove instrumental to achieve a more informed, hence more effective, therapeutic targeting. Since *ref* and *X1* isoforms are co-expressed across cancer types, our data also suggests generating and testing appropriate constructs in other experimental models of (*BRAFV600E*-driven) cancer types. Finally, it highlights the necessity to include untranslated regions, as they can heavily modify the biological outcome.

Transcending the boundaries of cancer biology, our findings indicate that *BRAF* gene has evolved significantly: the older *X1* protein is present in the ancient vertebrate lamprey, while the younger *ref* protein appears in marsupials (wallaby) (Additional file 1 : Fig. S6). Alternative splicing is a key component of biological complexity, and it is gaining momentum for its role in adaptation and evolution [10]. Therefore, we need to understand how and when *ref* isoform originated. We also need to discover the specific functions it carries out and whether its low levels represent a fail-safe mechanism, since it is so oncogenic when mutated.

Abbreviations

3'UTR	3'Untranslated region
cds	Coding sequence
dpf	Days post fertilization
FDA	Food and drug administration
hpf	Hours post fertilization
miRNA	MicroRNA

pA Poly A
RBP RNA binding protein
ref Reference

Supplementary Information

The online version contains supplementary material available at <https://doi.org/10.1186/s13578-023-01064-w>.

Additional file 1. Supplementary figures.

Additional file 2. Supplementary methods.

Additional file 3. Supplementary material. Sequence of ref cds, X1 cds, X2 cds, ref 3'UTR, X1 3'UTR.

Additional file 4. Supplementary Table 1. Primer sequence and use.

Acknowledgements

The authors thank M. Lanza, M.S. Podda together with all Poliseo lab members for helpful discussions. Authors also thank E. Guzzolino and A. Marranci for critical reading of the manuscript.

Author contributions

RDP, SS and LP conceived the project; RDP, SS, LeP and LP designed the experiments; RDP, SS, SB, FC and AT performed the experiments; all authors analyzed the data; LeP and LP supervised the research; RDP, AT and LP wrote the manuscript with the help of all authors. The manuscript was discussed and approved by all authors.

Funding

This work was supported by Istituto per lo Studio, la Prevenzione e la Rete Oncologica (institutional funding to LP). It was also partially supported by AIRC-Associazione Italiana Ricerca sul Cancro (MFAG #17095 and IG #25694 to LP).

Availability of data and materials

Not applicable.

Declarations

Ethics approval and consent to participate

Not applicable.

Consent for publication

Not applicable.

Competing interests

None to declare.

Received: 25 February 2023 Accepted: 5 June 2023

Published online: 01 July 2023

References

- Patton EE, Mueller KL, Adams DJ, Anandasabapathy N, Aplin AE, Bertolotto C, et al. Melanoma models for the next generation of therapies. *Cancer Cell*. 2021;39:610–31.
- Subbiah V, Baik C, Kirkwood JM. Clinical development of BRAF plus MEK inhibitor combinations. *Trends Cancer*. 2020;6:797–810.
- Marranci A, Jiang Z, Vitiello M, Guzzolino E, Comelli L, Sarti S, et al. The landscape of BRAF transcript and protein variants in human cancer. *Mol Cancer*. 2017;16:1.
- Fattore L, Mancini R, Acunzo M, Romano G, Lagana A, Pisanu ME, et al. miR-579-3p controls melanoma progression and resistance to target therapy. *Proc Natl Acad Sci USA* (Internet). 2016;113:E5005-13. Available from: <https://www.ncbi.nlm.nih.gov/pubmed/27503895>.

- Marranci A, D'Aurizio R, Vencken S, Mero S, Guzzolino E, Rizzo M, et al. Systematic evaluation of the microRNAome through miR-CATCHv2.0 identifies positive and negative regulators of BRAF-X1 mRNA. *RNA Biol*. 2019;16:1.
- Marranci A, Prantera A, Masotti S, De Paolo R, Baldanzi C, Podda MS, et al. PARP1 negatively regulates MAPK signaling by impairing BRAF-X1 translation. *J Hematol Oncol*. 2023;16:33.
- Lubrano S, Comelli L, Piccirilli C, Marranci A, Dapporto F, Tantillo E, et al. Development of a yeast-based system to identify new hBRAFF600E functional interactors. *Oncogene*. 2019;38:1.
- Patton EE, Widlund HR, Kutok JL, Kopani KR, Amatruda JF, Murphey RD, et al. BRAF mutations are sufficient to promote nevi formation and cooperate with p53 in the genesis of melanoma. *Curr Biol* (Internet). 2005/02/08. 2005;15:249–54. Available from: <http://www.ncbi.nlm.nih.gov/pubmed/15694309>.
- Erson-Bensan AE. RNA-biology ruling cancer progression? Focus on 3'UTRs and splicing. *Cancer Metastasis Rev*. 2020;39:887–901.
- Verta J-P, Jacobs A. The role of alternative splicing in adaptation and evolution. *Trends Ecol Evol*. 2022;37:299–308.

Publisher's Note

Springer Nature remains neutral with regard to jurisdictional claims in published maps and institutional affiliations.

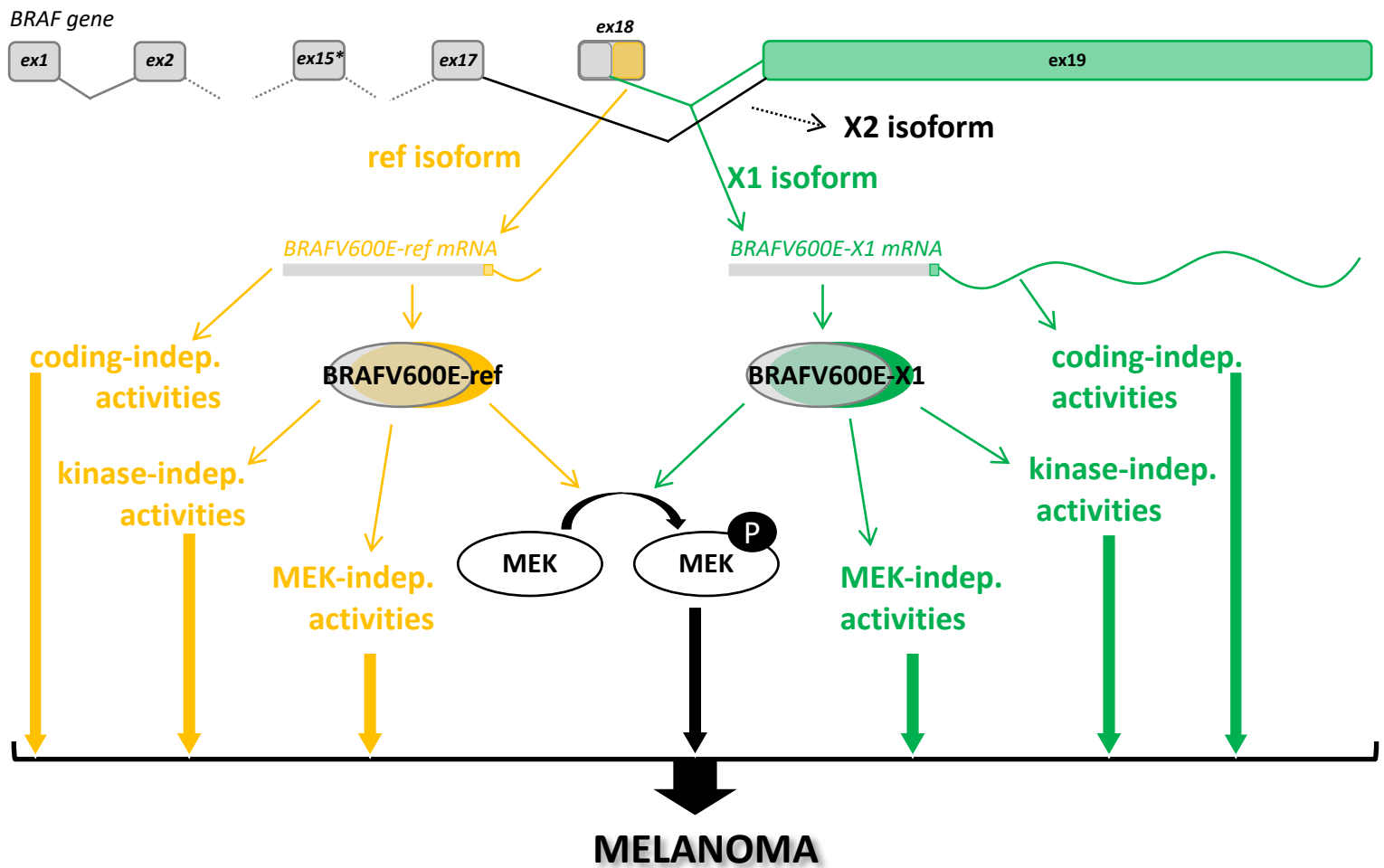
Ready to submit your research? Choose BMC and benefit from:

- fast, convenient online submission
- thorough peer review by experienced researchers in your field
- rapid publication on acceptance
- support for research data, including large and complex data types
- gold Open Access which fosters wider collaboration and increased citations
- maximum visibility for your research: over 100M website views per year

At BMC, research is always in progress.

Learn more biomedcentral.com/submissions

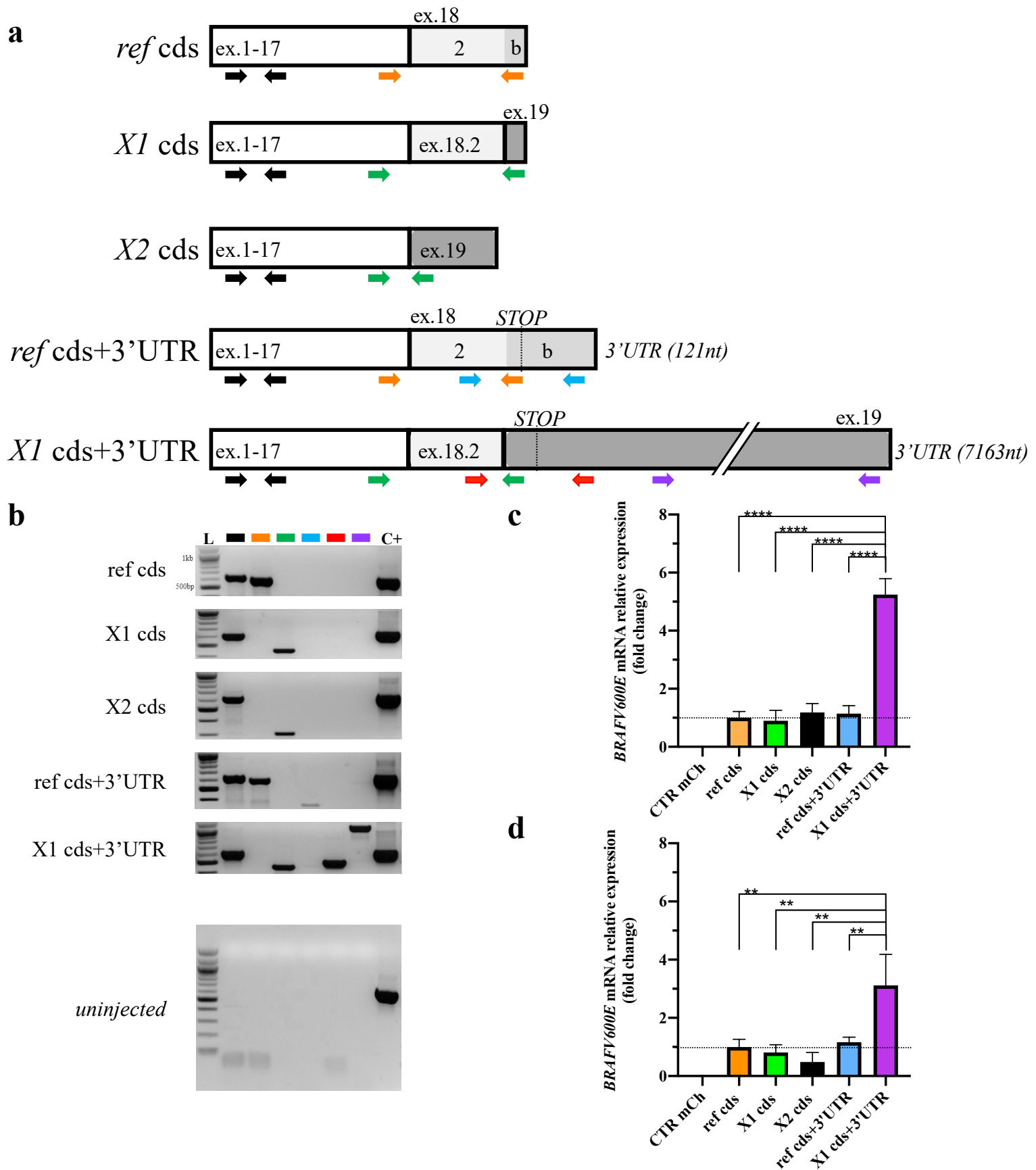




Supplementary Figure 1. Cartoon summarizing *BRAF* gene expression and functions.

The cartoon represents *BRAF* exons, as well as ref (yellow) and X1 (green) isoforms (mRNAs and proteins). In addition, the cartoon summarizes the functions possibly exerted by BRAF mRNA and protein isoforms, besides the well-known ability of BRAF kinase to phosphorylate MEK.

Exon 15, which encodes for the V600E mutation, is highlighted with an asterisk.

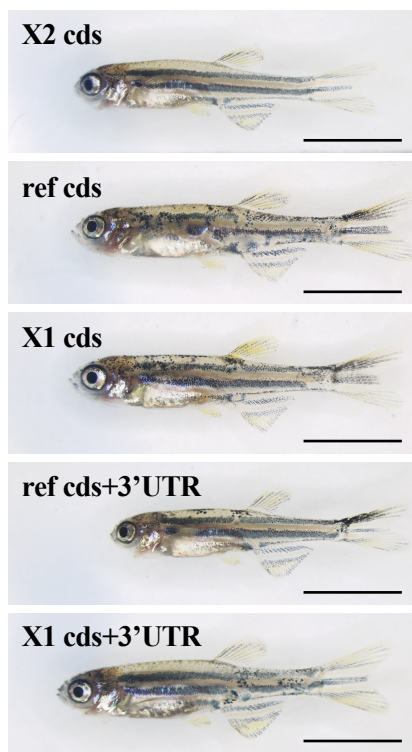


Supplementary Figure 2. Expression levels of *BRAFV600E* isoforms in *p53(lf)* embryos and larvae.

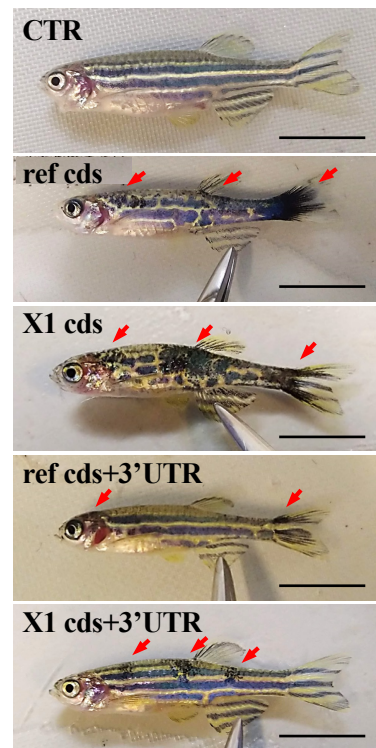
(a-b) PCR analysis. **(a)** Cartoon summarizing the position of PCR primers (colored arrows) used to determine the correct expression of cds and 3'UTR sequences of *BRAFV600E* mRNA isoforms. Exons (ex) are not in scale. **(b, upper)** Representative results of the PCR performed at 24hpf on *p53(lf)* embryos. These embryos were injected at 1-cell stage with the indicated plasmids. Primer pairs used are color-coded as in **a**. L: 100bp DNA ladder. C+: *actb1* exon-spanning primers are used as positive control. These primers amplify a 600bp band on cDNA and a 900bp band on genomic DNA. **(b, lower)** No PCR amplification, except for the positive control, are observed in uninjected *p53(lf)* embryos, ensuring the specificity of primer pairs for exogenous human *BRAF* over endogenous zebrafish *Braf*.

(c-d) qRT-PCR analysis. qRT-PCR was performed at 24hpf **(c)** and at 5dpf **(d)** on *p53(lf)* embryos/larvae injected at 1-cell stage with the indicated plasmids. *Tg(mitfa:mCherry,myl7:eGFP);p53(lf)* embryos/larvae are used as negative control. Data are expressed as mean \pm SEM. Differences were analyzed using one-way ANOVA (Tukey's) test. Statistically significant differences are indicated with asterisks: ** $P < 0.01$, **** $P < 0.0001$. qRT-PCR: quantitative Real Time Polymerase Chain Reaction; hpf: hours post fertilization; dpf: days post fertilization.

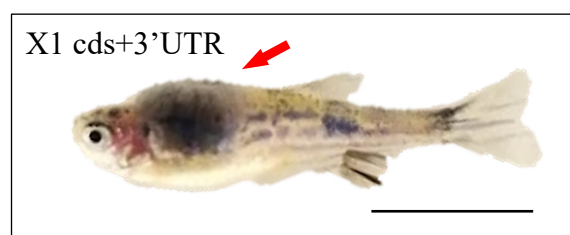
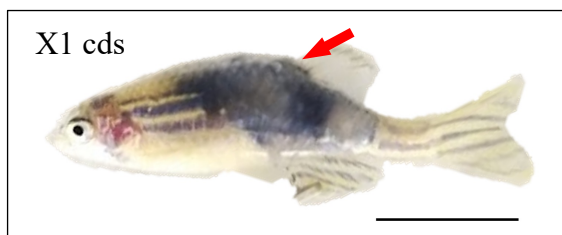
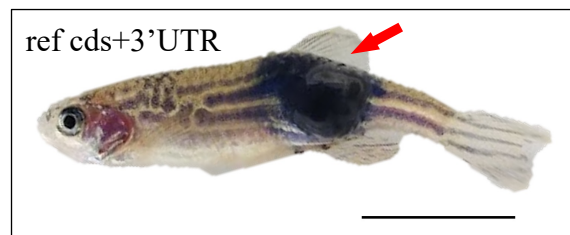
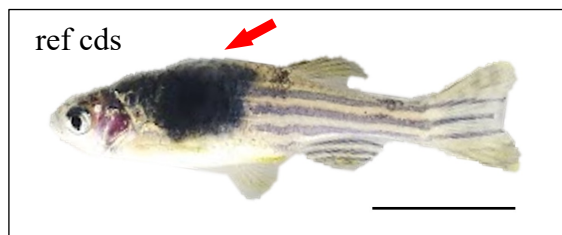
a



b



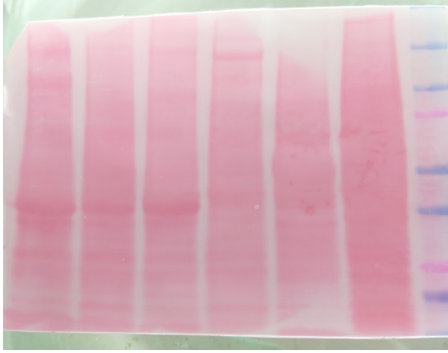
Supplementary Figure 3. Representative nevi in juvenile and adult *p53(lf)* fish injected with the indicated plasmids.
(a) Representative nevi in juvenile fish. A fish injected with X2 cds construct is used as negative control. Scale bar: 0.5cm.
(b) Representative nevi (red arrows) in adult fish (3 months of age). An uninjected fish is used as negative control (CTR). Scale bar: 1cm.



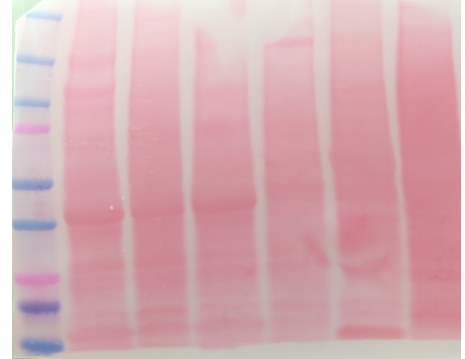
Supplementary Figure 4. Representative melanoma tumors in adult *p53(lf)* fish injected with the indicated plasmids. Tumors are indicated with red arrows. Scale bar: 1cm.

*protein extraction from melanoma tumors
(RIPA buffer)*

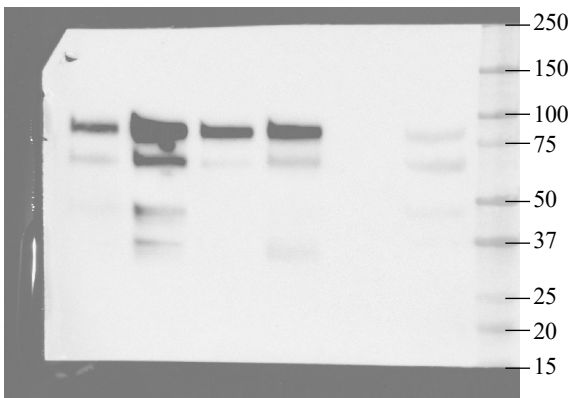
Gel #1



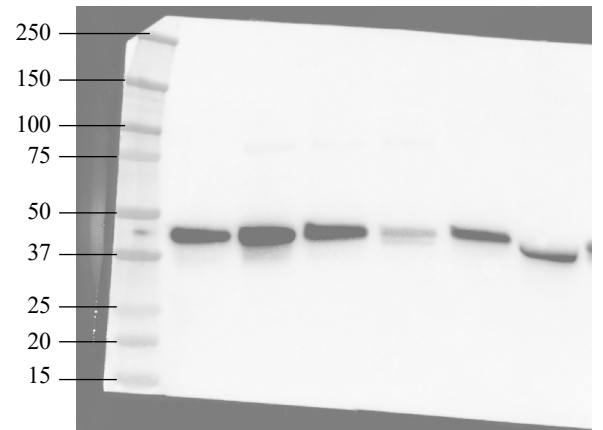
Gel #2



anti-BRAFV600E



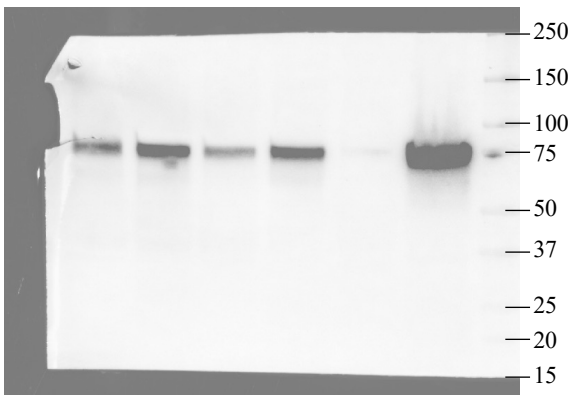
anti-p-Erk



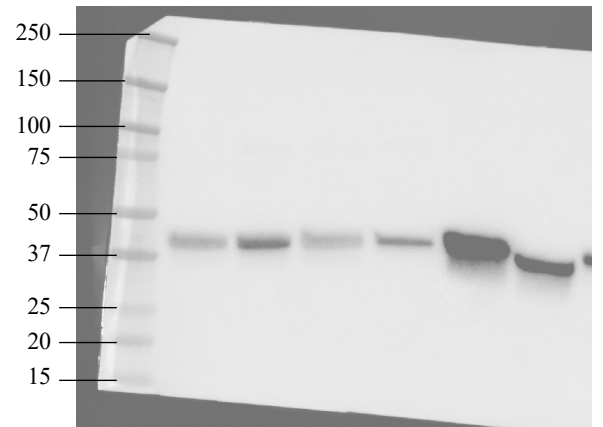
Stripping

(Restore™ Western Blot Stripping Buffer)

anti-Mcm7



anti-Erk



Supplementary Figure 5. Protein loading and whole blots of the western blot presented in Fig.1k.

a3' end of *BRAF* cds

Hsa ref-X1 comparison

<u>ENST00000646891.2</u>	AAACACCCATCCAGGCAGGGGGATATGGT	TGCGTTTCCTGTCCACTGA---
<u>ENST00000496384.7</u>	AAACACCCATCCAGGCAGGGGGATATGGG	AGAATTTGCAGCCTTCAAGTAG
	*****	* * * * *

Hsa/Laf/Meu ref comparison

<u>ENST00000646891.2</u>	AAACACCCATCCAGGCAGGGGGATATGGT	TGCGTTTCCTGTCCACTGA
<u>ENSLAFT00000016756.3</u>	AAACGCCCATCCAGGCAGGGGGCTACGGT	TGCGTTTCCTGTCCAC---
<u>ENSMEUG00000015422_ENSMEUT0000</u>	AAACGCCCATCCAGGCAGGGGGATATGGT	TGCGTTTCCTGTCCACTGA
	****	*****

Hsa/Mus/Dar/Pma X1 comparison

<u>ENST00000496384.7</u>	AAACACCCATCCAGGCAGGGGGATATGGG	AGAATTTGCAGCCTTCAAGTAG
<u>ENSMUST00000002487.15</u>	AAACACCCATCCAAGCAGGGGGATATGGG	AGAATTTGCAGCCTTCAAGTAG
<u>ENSDART00000023894.11</u>	AAACACCCATTTCAGGCCGGTGGCTATGGT	TGAATTCACAGCGTTTAAATAG
<u>ENSPMAG00000005000_ENSPMAT0000</u>	GGACCCCGATCCAGGCAGGGCGGATACGGG	AGAGTTTGCAGCCTTCAAGTAG
	* * * * *	* * * * *

b

C-terminal of BRAF protein

Hsa ref-X1 comparison

<u>ENST00000646891.2</u>	ARSLPKIHRSAEPSLNRAGFQTEDFSLYACASPKTPIQAGGY	GAFPVH-
<u>ENST00000496384.7</u>	ARSLPKIHRSAEPSLNRAGFQTEDFSLYACASPKTPIQAGGY	GEFAAFK
	*****	* ..

Hsa/Laf/Meu ref comparison

<u>ENST00000646891.2</u>	ARSLPKIHRSAEPSLNRAGFQTEDFSLYACASPKTPIQAGGY	GAFPVH
<u>ENSLAFT00000016756.3</u>	ARSLPKIHRSAEPSLNRAGFQTEDFSLYACASPKTPIQAGGY	GAFPVH
<u>ENSMEUG00000015422_ENSMEUT0000</u>	ARSLPKIHRSAEPSLNRAGFQTEDFSLYACASPKTPIQAGGY	GAFPVH
	*****	*****

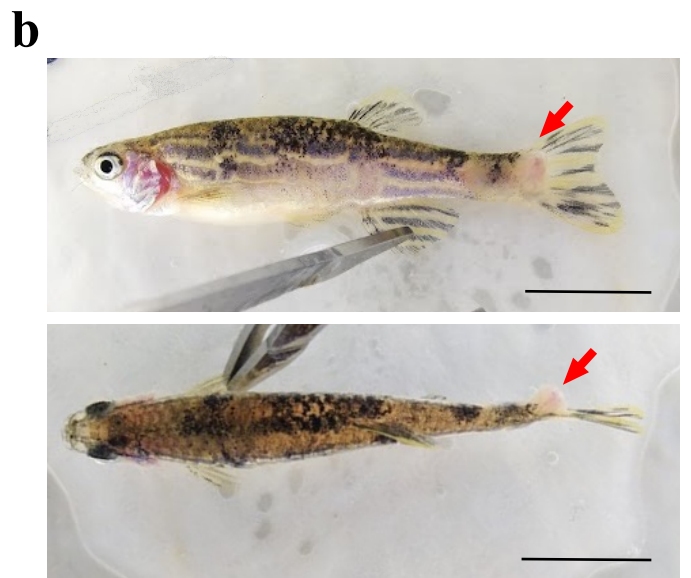
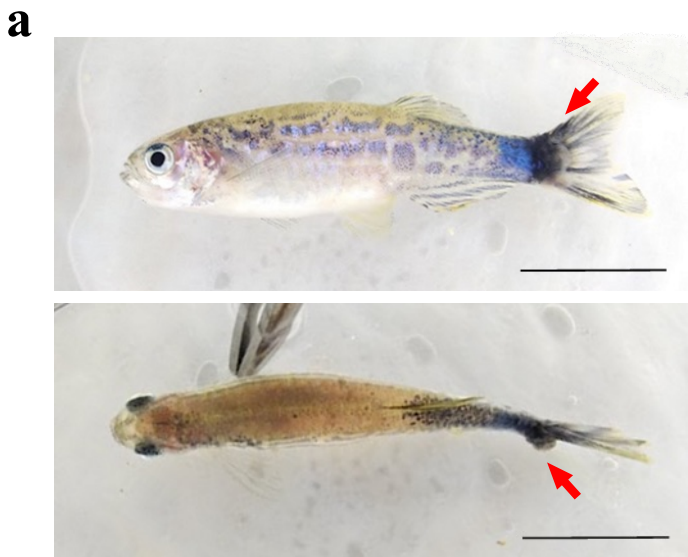
Hsa/Mus/Dar/Pma X1 comparison

<u>ENST00000496384.7</u>	ARSLPKIHRSAEPSLNRAGFQTEDFSLYACASPKTPIQAGGY	GEFAAFK
<u>ENSMUST00000002487.15</u>	ARSLPKIHRSAEPSLNRAGFQTEDFSLYACASPKTPIQAGGY	GEFAAFK
<u>ENSDART00000023894.11</u>	ARSLPKIHRSAEPSLNRAGFQTEDFSLYTCASPKTPIQAGGY	GEFTAFK
<u>ENSPMAG00000005000_ENSPMAT0000</u>	ARSLPKIHRSAEPSLNRAGFQTDFFSSYT CASPRTP IQAGGY	GEFAAFK
	*****	:*** *:***:*****:***

Supplementary Figure 6. Alignment of the 3' end of *BRAF* cds and the C-terminal of BRAF protein.

(a) Alignment of the 3' end of *BRAF* cds. *Upper*: alignment of *ref* (yellow underline) and *X1* (green underline) sequence of human *BRAF*. *Middle*: alignment of human *BRAF-ref* (yellow underline; *Homo sapiens* Hsa) with elephant *Braf* (*Loxodonta africana* Laf) and wallaby *Braf* (*Macropus eugenii* Meu). *Lower*: alignment of human *BRAF-X1* (green underline; *Homo sapiens* Hsa) with mouse *Braf* (*Mus musculus* Mus), zebrafish *braf* (*Danio rerio* Dar), and lamprey *braf* (*Petromyzon marinus* Pma). The boxes on the right highlight that DNA/RNA sequences are not conserved.

(b) Alignment of the C-terminal of BRAF protein. *Upper*: alignment of *ref* (yellow underline) and *X1* (green underline) sequence of human BRAF. *Middle*: alignment of human BRAF-*ref* (yellow underline; *Homo sapiens* Hsa) with elephant BRAF (*Loxodonta africana* Laf) and wallaby BRAF (*Macropus eugenii* Meu). *Lower*: alignment of human BRAF-X1 (green underline) with mouse *Braf* (*Mus musculus* Mus), zebrafish *Braf* (*Danio rerio* Dar), and lamprey *Braf* (*Petromyzon marinus* Pma). The boxes on the right highlight the differences in protein sequence between human *ref* and *X1* isoforms, the conservation of *ref* protein isoform in mammals across wallaby, elephant and human, as well as the conservation of *X1* protein isoform outside mammals and across lamprey, zebrafish, mouse, and human.



Supplementary Figure 7. Phenotypic analysis.

(a) Representative example of a melanotic tumor (red arrow) in lateral (*upper*) and dorsal (*lower*) view. Scale bar: 1cm.

(b) Representative example of an amelanotic tumor (red arrow) in lateral (*upper*) and dorsal (*lower*) view. Scale bar: 1cm.

SUPPLEMENTARY METHODS

Zebrafish husbandry

The zebrafish facility at CNR-IFC has been authorized by the Italian Ministry of Health (authorization #297/2012-A, issued on December 21, 2012) and by the Municipality of Pisa (authorization #DN-16/504, issued on June 7, 2013). Zebrafish (*Danio rerio*) experiments were carried out in accordance with the European Union guidelines for animal welfare [European Communities Council Directive of September 22, 2010 (2010/63/ UE)]. All experimental protocols were approved by the Italian Ministry of Health (authorization #383/2020-PR). Zebrafish were raised and maintained on a 14h/10h light/dark cycle at 28.5°C, in a zebrafish housing system (Tecniplast) under pH- and salinity-controlled conditions. Embryos were obtained by natural spawning, were maintained in E3 medium (5mM NaCl, 0.17mM KCl, 0.33mM CaCl₂, 0.33mM MgSO₄, 10⁻⁵ % methylene blue), and were staged according to hours post fertilization (hpf) and morphologic criteria [1]. Embryos euthanasia was performed by hypothermia shock for at least 20 minutes, while adults were euthanized by exposure to excess of tricaine methanesulfonate (MS-222, #A5040, Sigma).

Plasmid cloning

The plasmids injected in zebrafish embryos are the following:

pDEST(*mitfa*:-2.3Hsa.BRAF_V600E-220,*myl7*:eGFP) for the expression of BRAFV600E-ref cds;
pDEST(*mitfa*:-2.3Hsa.BRAF_V600E-204,*myl7*:eGFP) for the expression of BRAFV600E-X1 cds;
pDEST(*mitfa*:-2.3Hsa.BRAF_V600E-X2,*myl7*:eGFP) for the expression of BRAFV600E-X2 cds;
pDEST(*mitfa*:-2.4Hsa.BRAF_V600E-220,*myl7*:eGFP) for the expression of BRAFV600E-ref cds+3'UTR;
pDEST(*mitfa*:-9.4Hsa.BRAF_V600E-204,*myl7*:eGFP) for the expression of BRAFV600E-X1 cds+3'UTR.

They were generated using Tol2kit (http://tol2kit.genetics.utah.edu/index.php/Main_Page).

In brief, the cds sequence of human *BRAF* isoforms carrying the activating V600E mutation was amplified by PCR from PIG-BRAFV600E-ref, X1, and X2 plasmids [2]; the ref 3'UTR sequence was amplified from pMIR-ref-3'UTR [3]; the X1 3'UTR sequence was amplified from pCW-X1-3'UTR plasmid. In turn, pCW-X1-3'UTR plasmid was obtained by PCR amplification of the X1 3'UTR from A375 genomic DNA using 7kb_X1_3UTR_Fw (Sall STOP) primer (5' agcgtcgacTAGCCACCATCATGGCAG 3') and 7kb_X1_3UTR_Rv (Mlul) primer (5' CAGACGCGTttctcctatcgactcaatcttta 3'), and subsequent cloning in the pCW backbone [3] using Sall and Mlul restriction enzymes. All human *BRAF* sequences are listed in **Supplementary material**. PCR amplicons were then inserted into the multiple cloning site of pME-MCS plasmid (Tol2kit), using Sall-SpeI and SpeI-NotI restriction sites. To create pDEST plasmids, pME-*BRAF* plasmids were mixed with p5E-*mitfa* promoter plasmid (kind gift from Dr. Charles Kaufman, Washington University School of Medicine, St. Louis, USA), p3E-polyA plasmid (Tol2kit), and pDestTol2CG* backbone plasmid (Tol2kit), in presence of Gateway™ LR Clonase™ Enzyme (Thermo Fisher Scientific), as reported in [4].

PCR reactions involved in cloning were performed using Phusion Flash High-Fidelity PCR Master Mix (Thermo Fisher Scientific) and the primers listed in **Suppl. Table 1**. PCR amplicons were run on a 0.8-2% agarose gel and extracted using QIAquick Gel Extraction Kit (Qiagen). Successful cloning was confirmed subjecting plasmids to Sanger sequencing (Eurofins Genomics).

Plasmid microinjection in 1-cell stage zebrafish embryos

Zebrafish of the *p53(lf)* strain (ZDB-ALT-050428-2) (kind gift from Dr. Francesco Argenton, Università di Padova) were bred and embryos were collected for microinjection. 25pg of plasmidic DNA and 25pg of *Tol2* mRNA were coinjected into 1-cell stage embryos for the biggest plasmid (pDEST(*mitfa*:-9.4Hsa.BRAF_V600E-204,*myl7*:eGFP)). Following the calculation of molar concentration, equimolar amounts of the other pDEST plasmids were microinjected. After microinjection, embryos were maintained in E3 medium at 28.5°C. At 24-48hpf they were selected based on heart-specific green fluorescence, using MZ10F Leica stereomicroscope. Successfully injected embryos were then subjected to further analysis, as described below.

Zebrafish imaging and phenotypic analysis

5dpf larvae were anesthetized and immersed in methylcellulose. Images were acquired using M80 Leica stereomicroscope, equipped with a Nikon DS-Fi1 camera.

Juvenile and adult fish were anesthetized, and images were acquired in water using M80 Leica stereomicroscope or ASUS Zenfone X00TD camera.

Nevi were defined as flat, strongly pigmented clusters of melanocytes that disrupt the distinctive striping pattern [5] [6]. Quantification of nevus area was performed using ImageJ software (<http://rsb.info.nih.gov>). For each animal, pictures of the lateral (right and left) and dorsal positions were analyzed. The area of the nevi visible in each picture was measured with ImageJ. Then, the biggest area for each animal was included in the graph and subjected to statistical analysis.

The transition from nevus to melanoma was detected as pigmentation intensification, which turns into skin thickening, accompanied by outward growth [7]. Melanoma tumors were defined as melanotic/amelanotic based on the presence/absence of pigmentation according to visual inspection (see **Suppl. Fig.7** for an example).

Melanoma-free survival curves

Adult animals up to 50 weeks old were checked weekly for the presence of melanoma tumors and Kaplan-Meier curves for melanoma-free survival were created.

Collection, RNA extraction and retrotranscription of embryos and larvae

Embryos and larvae (at least 20 per experimental condition) were homogenized by insulin needle. Total RNA was extracted using QIAzol (Qiagen) following the manufacturer's instructions, quantified using Nanodrop Lite (Thermo Fisher Scientific), verified on 2% agarose gel and reverse transcribed with the SuperScript III RT reaction kit (Thermo Fisher Scientific) following the manufacturer's instructions. The successful retrotranscription and the absence of contaminating genomic DNA were routinely checked through a control PCR (PCR Master Mix, Thermo Fisher Scientific) in which the exon-spanning primers for *actb1* mRNA are used.

RT-PCR of embryos

To detect the expression of *BRAFV600E* isoforms from pDEST plasmids (see above), GoTaq® G2 Green Master Mix (PROMEGA) was used with 10ng of cDNA, 0.5µM primers and 58°C annealing temperature. The primers list is reported in **Suppl. Table 1**.

qRT-PCR of embryos and larvae

Quantitative analysis of *BRAFV600E* isoforms expression from pDEST plasmids (see above) was performed in triplicate with SSOADV Universal SYBR Green (Bio-Rad) in 15µl final reaction volume on a CFX96 Real-Time System (Bio-Rad). 37.5ng of cDNA, 0.5µM primers and 60°C annealing temperature were used. The primers list is reported in **Suppl. Table 1**.

PCR efficiency and expression data were analyzed using CFX Manager Software (Bio-Rad). Relative expression of *BRAFV600E* isoforms was determined using the $2^{-\Delta\Delta C_t}$ method and data were normalized using housekeeping genes (*ef1a1/1*, *actb1*) [3].

Collection and histological analysis of melanoma specimens

Three weeks after tumor onset, fish were euthanized, then fixed in 4% PFA for 48h at 4°C, dehydrated through a series of graded ethanol baths, and finally embedded in paraffin. Transverse paraffin-embedded tissue sections (5µm) were used. Hematoxylin and Eosin (H&E) staining was carried out using standard methods. For immunohistochemistry (IHC) analysis, tissue sections were stained using standard whole-mount immunostaining protocol with Vectastain elite ABC kit (Vector Laboratories) and 1:50 mouse anti-BRAFV600E primary antibody (#ab228461, clone VE1, Abcam).

Collection and western blot analysis of melanoma specimens

Three weeks after tumor onset, fish were euthanized, and tumors were isolated. They were then homogenized with a pestle for 15-30 minutes, while kept on ice in 50-100µL of RIPA Buffer (50mM Tris HCl, 150mM NaCl, 0.5% NaDeoxycholate, 0.1% SDS, 1% NP40) supplemented with 1mM PMSF, 2mM Na orthovanadate, and cOmplete™ Protease Inhibitor (Roche). The mixture was centrifuged at 14000rpm for 30min at 4°C and the supernatant was quantified using BCA reagent (#23227, Thermo Fisher Scientific) at 590nm. 30µg of proteins were combined with 4X loading buffer

(Bio-Rad), heated at 95°C for 5min, and loaded on a 4-15% SDS-polyacrylamide gel (Mini-PROTEAN Precast gel, BioRad) along with a molecular weight marker (Bio-Rad). Proteins were then electrotransferred to a polyvinylidene difluoride (PVDF) membrane using Trans-Blot Turbo system (Bio-Rad). Membranes were blocked at room temperature for 1h using 5% milk in TBST. They were then incubated overnight at 4°C with the following primary antibodies:

-mouse anti-BRAFV600E VE1 antibody ((#ab228461, clone VE1, Abcam; 1:400 dilution in 1% BSA in TBST);

-mouse anti-MCM7 monoclonal antibody (#sc-9966, clone 141.2, Santa Cruz Biotechnology; 1:200 dilution in 1% BSA in TBST);

-mouse anti-p-ERK 1/2 monoclonal antibody (#sc-7383, clone E-4, Santa Cruz Biotechnology; 1:500 dilution in 3% BSA in TBST);

-mouse anti-ERK 2 polyclonal antibody (#sc-1647, clone D-2, Santa Cruz Biotechnology; 1:500 dilution in 3% BSA in TBST).

Blots were washed 4 x 5min in TBST and incubated for 1h with the appropriate secondary antibody (1:3000 dilution in 5% milk in TBST). Blots were again washed 4 x 5min in TBST and developed using Clarity Western ECL blotting substrate (Bio-Rad). Finally, bands were detected using ChemiDoc imaging system (Bio-Rad). Membrane stripping was performed using Restore™ Western Blot Stripping Buffer (#21059, Thermo Fisher Scientific).

Statistical analyses

Data were analyzed according to their normality using parametric or non-parametric tests. qRT-PCR data were analyzed using one-way ANOVA (Tukey's) test. Nevus percentage and tumor macro-features were analyzed using Fisher's exact test. Nevus size was analyzed using Kruskal-Wallis (Dunn's) test. Kaplan-Meier curves were analyzed using log-rank (Mantel-Cox) test. When appropriate, data are expressed as mean ± SEM (standard error of the mean). $p < 0.05$ was taken as a minimum level of significance. To account for biological and technical variability, at least 2 independent biological replicates were performed for each experiment. The total number of juvenile or adult fish studied for each experimental condition is reported in each graph.

REFERENCES

1. Kimmel CB, Ballard WW, Kimmel SR, Ullmann B, Schilling TF. Stages of embryonic development of the zebrafish. *Developmental Dynamics*. 1995;203:253–310.
2. Marranci A, Jiang Z, Vitiello M, Guzzolino E, Comelli L, Sarti S, et al. The landscape of BRAF transcript and protein variants in human cancer. *Mol Cancer*. 2017;16.
3. Marranci A, D'Aurizio R, Vencken S, Mero S, Guzzolino E, Rizzo M, et al. Systematic evaluation of the microRNAome through miR-CATCHv2.0 identifies positive and negative regulators of BRAF-X1 mRNA. *RNA Biol*. 2019;16.
4. Sarti S, De Paolo R, Ippolito C, Pucci A, Pitto L, Poliseno L. Inducible modulation of miR-204 levels in a zebrafish melanoma model. *Biol Open*. 2020;9.
5. Patton EE, Widlund HR, Kutok JL, Kopani KR, Amatruda JF, Murphey RD, et al. BRAF mutations are sufficient to promote nevi formation and cooperate with p53 in the genesis of melanoma. *Curr Biol* [Internet]. 2005/02/08. 2005;15:249–54. Available from: <http://www.ncbi.nlm.nih.gov/pubmed/15694309>
6. Dovey M, White RM, Zon LI. Oncogenic NRAS Cooperates with p53 Loss to Generate Melanoma in Zebrafish. *Zebrafish*. 2009;6:397–404.
7. Patton EE, Mathers ME, Scharf M. Generating and analyzing fish models of melanoma. *Methods Cell Biol* [Internet]. 2011;105:339–66. Available from: <https://www.ncbi.nlm.nih.gov/pubmed/21951537>

SUPPLEMENTARY MATERIAL. Sequence of ref cds, X1 cds, X2 cds, ref 3'UTR, X1 3'UTR.

	Sequence 5' → 3'
hBRAF-ref cds (NM_004333.6)	<p>ATGGCGGCGCTGAGCGGTGGCGGTGGTGGCGGCGCGGAGCCGG GCCAGGCTCTGTTCAACGGGGACATGGAGCCCAGGCCGGCGCC GGCGCCGGCGCCGCGGCCTCTTCGGCTGCGGACCCTGCCATTCC GGAGGAGGTGTGGAATATCAAACAAATGATTAAGTTGACACAGGAA CATATAGAGGCCCTATTGGACAAATTTGGTGGGGAGCATAATCCAC CATCAATATATCTGGAGGCCTATGAAGAATACACCAGCAAGCTAGA TGCACTCCAACAAAGAGAACAACAGTTATTGGAATCTCTGGGGAAC GGAAGTGAATTTTTCTGTTTCTAGCTCTGCATCAATGGATACCGTTAC ATCTTCTTCTCTTCTAGCCTTTCAGTGCTACCTTCATCTCTTTTCACT TTTTCAAATCCCACAGATGTGGCACGGAGCAACCCCAAGTCACCA CAAAAACCTATCGTTAGAGTCTTCCCTGCCCAACAACAGAGGACAG TGGTACCTGCAAGGTGTGGAGTTACAGTCCGAGACAGTCTAAGAA AGCACTGATGATGAGAGGTCTAATCCCAGAGTGTGTGCTGTTTAC AGAATTCAGGATGGAGAGAAGAAACCAATTGGTTGGGACACTGATA TTTCCCTGGCTTACTGGAGAAGAATTGCATGTGGAAGTGTGGAGAA TGTTCCACTTACAACACACAACCTTTGTACGAAAACGTTTTTCCACT TAGCATTGTTGACTTTTGTGCGAAAGCTGCTTTTCCAGGGTTTCCGC TGTCAAACATGTGGTTATAAATTTACCAGCGTTGTAGTACAGAAGT TCCACTGATGTGTGTTAATTATGACCAACTTGATTTGCTGTTTGTCT CCAAGTTCTTTGAACACCACCCAATACCACAGGAAGAGGCGTCTT AGCAGAGACTGCCCTAACATCTGGATCATCCCCTTCCGCACCCGC CTCGGACTCTATTGGGCCCAAATTCTCACCAGTCCGTCTCCTTCA AAATCCATTCCAATTCCACAGCCCTTCCGACCAGCAGATGAAGATC ATCGAAATCAATTTGGGCAACGAGACCGATCCTCATCAGCTCCCAA TGTGCATATAAACACAATAGAACCTGTCAATATTGATGACTTGATTA GAGACCAAGGATTTCTGTTGATGGAGGATCAACCACAGGTTTGTCT TGCTACCCCCCTGCCTCATTACCTGGCTCACTAACTAACGTGAAA GCCTTACAGAAATCTCCAGGACCTCAGCGAGAAAGGAAGTCATCTT CATCCTCAGAAGACAGGAATCGAATGAAAACACTTGGTAGACGGGA CTCGAGTGATGATTGGGAGATTCCTGATGGGCAGATTACAGTGGG ACAAAGAATTGGATCTGGATCATTGGAACAGTCTACAAGGGAAAG TGGCATGGTGATGTGGCAGTGAAAATGTTGAATGTGACAGCACCTA CACCTCAGCAGTTACAAGCCTTCAAAAATGAAGTAGGAGTACTCAG GAAAACACGACATGTGAATATCCTACTTTCATGGGCTATTCCACAA AGCCACAACCTGGCTATTGTTACCCAGTGGTGTGAGGGCTCCAGCTT GTATCACCATCTCCATATCATTGAGACCAAATTTGAGATGATCAAAC TTATAGATATTGCACGACAGACTGCACAGGGCATGGATTACTTACA CGCCAAGTCAATCATCCACAGAGACCTCAAGAGTAATAATATATTTT TTCATGAAGACCTCACAGTAAAATAGGTGATTTTGGTCTAGCTACA GTGAAATCTCGATGGAGTGGGTCCCATCAGTTTGAACAGTTGTCTG GATCCATTTTGTGGATGGCACCAGAAGTCATCAGAATGCAAGATAA AAATCCATACAGCTTTCAGTCAGATGTATATGCATTTGGGATTGTTT TGTATGAATTGATGACTGGACAGTTACCTTATTCAAACATCAACAAC AGGGACCAGATAATTTTTATGGTGGGACGAGGATACCTGTCTCCAG ATCTCAGTAAGGTACGGAGTAACTGTCCAAAAGCCATGAAGAGATT AATGGCAGAGTGCCTCAAAAAGAAAAGAGATGAGAGACCACTCTTT CCCCAAATTCTCGCCTCTATTGAGCTGCTGGCCCGCTCATTGCCAA AAATTCACCGCAGTGCATCAGAACCCTCCTTGAATCGGGCTGGTTT CCAAACAGAGGATTTTAGTCTATATGCTTGTGCTTCTCCAAAACAC CCATCCAGGCAGGGGGATATGGTGCCTTCTGTCCACTGA</p>
hBRAF-X1 cds (NM_001354609.2)	<p>ATGGCGGCGCTGAGCGGTGGCGGTGGTGGCGGCGCGGAGCCGG GCCAGGCTCTGTTCAACGGGGACATGGAGCCCAGGCCGGCGCC GGCGCCGGCGCCGCGGCCTCTTCGGCTGCGGACCCTGCCATTCC</p>

	<p>GGAGGAGGTGTGGAATATCAAACAAATGATTAAGTTGACACAGGAA CATATAGAGGCCCTATTGGACAAATTTGGTGGGGAGCATAATCCAC CATCAATATATCTGGAGGCCTATGAAGAATACACCAGCAAGCTAGA TGCACTCCAACAAAGAGAACAACAGTTATTGGAATCTCTGGGGAAC GGAAGTGAATTTTTCTGTTTCTAGCTCTGCATCAATGGATACCGTTAC ATCTTCTTCTTCTTAGCCTTTCAGTGCTACCTTCATCTCTTTTCACT TTTTCAAATCCCACAGATGTGGCACGGAGCAACCCCAAGTCACCA CAAAAACCTATCGTTAGAGTCTTCTGCCCCAACAAACAGAGGACAG TGGTACCTGCAAGGTGTGGAGTTACAGTCCGAGACAGTCTAAAGAA AGCACTGATGATGAGAGGTCTAATCCCAGAGTGTGTGCTGTTTAC AGAATTCAGGATGGAGAGAAGAAACCAATTGGTTGGGACACTGATA TTTCTGGCTTACTGGAGAAGAATTGCATGTGGAAGTGTGGAGAA TGTTCCACTTACAACACACAACCTTTGTACGAAAAACGTTTTTCACT TAGCATTGTTGACTTTTGTGCGAAAGCTGCTTTTCCAGGGTTTCCGC TGTCAAACATGTGGTTATAAATTTACCAGCGTTGTAGTACAGAAGT TCCACTGATGTGTGTTAATTATGACCAACTTGATTTGCTGTTTGTCT CCAAGTTCTTTGAACACCACCCAATACCACAGGAAGAGGCGTCTT AGCAGAGACTGCCCTAACATCTGGATCATCCCCTTCCGCACCCGC CTCGGACTCTATTGGGCCCAAATTCTCACCAGTCCGTCTCCTTCA AAATCCATTCCAATTCCACAGCCCTTCCGACCAGCAGATGAAGATC ATCGAAATCAATTTGGGCAACGAGACCGATCCTCATCAGCTCCCAA TGTGCATATAAACACAATAGAACCTGTCAATATTGATGACTTGATTA GAGACCAAGGATTTCTGTTGATGGAGGATCAACCACAGGTTTGTCT TGCTACCCCCCTGCCTCATTACCTGGCTCACTAACTAACGTGAAA GCCTTACAGAAATCTCCAGGACCTCAGCGAGAAAGGAAGTCATCTT CATCCTCAGAAGACAGGAATCGAATGAAAACACTTGGTAGACGGGA CTCGAGTGATGATTGGGAGATTCCTGATGGGCAGATTACAGTGGG ACAAAGAATTGGATCTGGATCATTGGAACAGTCTACAAGGGAAAG TGGCATGGTGTGTGGCAGTGAAAATGTTGAATGTGACAGCACCTA CACCTCAGCAGTTACAAGCCTTCAAAAATGAAGTAGGAGTACTCAG GAAAACACGACATGTGAATATCCTACTCTTCATGGGCTATTCCACAA AGCCACAACCTGGCTATTGTTACCCAGTGGTGTGAGGGCTCCAGCTT GTATCACCATCTCCATATCATTGAGACCAAATTTGAGATGATCAAAC TTATAGATATTGCACGACAGACTGCACAGGGCATGGATTACTTACA CGCCAAGTCAATCATCCACAGAGACCTCAAGAGTAATAATATATTTT TTCATGAAGACCTCACAGTAAAATAGGTGATTTTGGTCTAGCTACA GAGAAATCTCGATGGAGTGGGTCCCATCAGTTTGAACAGTTGTCTG GATCCATTTTGTGGATGGCACCAGAAGTCATCAGAATGCAAGATAA AAATCCATACAGCTTTCAGTCAGATGTATATGCATTTGGGATTGTTT TGTATGAATTGATGACTGGACAGTTACCTTATTCAAACATCAACAAC AGGGACCAGATAATTTTTATGGTGGGACGAGGATACCTGTCTCCAG ATCTCAGTAAGGTACGGAGTAAGTGTCCAAAAGCCATGAAGAGATT AATGGCAGAGTGCCTCAAAAAGAAAAGAGATGAGAGACCACTCTTT CCCCAAATTCTCGCCTCTATTGAGCTGCTGGCCCGCTCATTGCCAA AAATTCACCGCAGTGCATCAGAACCCTCCTTGAATCGGGCTGGTTT CAAACAGAGGATTTTAGTCTATATGCTTGTGCTTCTCCAAAACAC CCATCCAGGCAGGGGGATATGGAGAATTTGCAGCCTTCAAGTAG</p>
<p>hBRAf-X2 cds (NM_001378468.1)</p>	<p>ATGGCGGCGCTGAGCGGTGGCGGTGGTGGCGGCGCGGAGCCGG GCCAGGCTCTGTTCAACGGGGACATGGAGCCCAGGCCGGCGCC GGCGCCGGCGCCGCGGCCTCTTCGGCTGCGGACCCTGCCATTCC GGAGGAGGTGTGGAATATCAAACAAATGATTAAGTTGACACAGGAA CATATAGAGGCCCTATTGGACAAATTTGGTGGGGAGCATAATCCAC CATCAATATATCTGGAGGCCTATGAAGAATACACCAGCAAGCTAGA TGCACTCCAACAAAGAGAACAACAGTTATTGGAATCTCTGGGGAAC GGAAGTGAATTTTTCTGTTTCTAGCTCTGCATCAATGGATACCGTTAC ATCTTCTTCTTCTTAGCCTTTCAGTGCTACCTTCATCTCTTTTCACT</p>

	<p>TTTTCAAATCCCACAGATGTGGCACGGAGCAACCCCAAGTCACCA CAAAAACCTATCGTTAGAGTCTTCCTGCCAACAAACAGAGGACAG TGGTACCTGCAAGGTGTGGAGTTACAGTCCGAGACAGTCTAAAGAA AGCACTGATGATGAGAGGTCTAATCCCAGAGTGTCTGTGCTGTTTAC AGAATTCAGGATGGAGAGAAGAAACCAATTGGTTGGGACACTGATA TTTCCTGGCTTACTGGAGAAGAATTGCATGTGGAAGTGTGGAGAA TGTTCCACTTACAACACACAACCTTTGTACGAAAAACGTTTTTCACCT TAGCATTTTGTGACTTTTGTGCGAAAGCTGCTTTTCCAGGGTTTCCGC TGTCAAACATGTGGTTATAAATTTACCAGCGTTGTAGTACAGAAGT TCCACTGATGTGTGTTAATTATGACCAACTTGATTTGCTGTTTGTCT CCAAGTTCTTTGAACACCACCCAATACCACAGGAAGAGGCGTCCCT AGCAGAGACTGCCCTAACATCTGGATCATCCCCTTCCGCACCCGC CTCGGACTCTATTGGGCCCAAATTCTCACCAGTCCGTCTCCTTCA AAATCCATTCCAATTCCACAGCCCTTCCGACCAGCAGATGAAGATC ATCGAAATCAATTTGGGCAACGAGACCGATCCTCATCAGCTCCCAA TGTGCATATAAACACAATAGAACCTGTCAATATTGATGACTTGATTA GAGACCAAGGATTTCTGGTGTGATGGAGGATCAACCACAGGTTTGTG TGCTACCCCCCTGCCTCATTACCTGGCTCACTAACTAACGTGAAA GCCTTACAGAAATCTCCAGGACCTCAGCGAGAAAGGAAGTCATCTT CATCCTCAGAAGACAGGAATCGAATGAAAACACTTGGTAGACGGGA CTCGAGTGATGATTGGGAGATTCCTGATGGGCAGATTACAGTGGG ACAAAGAATTGGATCTGGATCATTGGAACAGTCTACAAGGGAAAG TGGCATGGTGTGATGTGGCAGTGAAAATGTTGAATGTGACAGCACCTA CACCTCAGCAGTTACAAGCCTTCAAAAATGAAGTAGGAGTACTCAG GAAAACACGACATGTGAATATCCTACTCTTCATGGGCTATTCCACAA AGCCACAACCTGGCTATTGTTACCCAGTGGTGTGAGGGCTCCAGCTT GTATCACCATCTCCATATCATTGAGACCAAATTTGAGATGATCAAAC TTATAGATATTGCACGACAGACTGCACAGGGCATGGATTACTTACA CGCCAAGTCAATCATCCACAGAGACCTCAAGAGTAATAATATATTTT TTCATGAAGACCTCACAGTAAAATAGGTGATTTTGGTCTAGCTACA GTGAAATCTCGATGGAGTGGGTCCCATCAGTTTGAACAGTTGTCTG GATCCATTTTGTGGATGGCACCAGAAGTCATCAGAATGCAAGATAA AAATCCATACAGCTTTCAGTCAGATGTATATGCATTTGGAATTGTTT TGTATGAATTGATGACTGGACAGTTACCTTATTCAAACATCAACAAC AGGGACCAGATAATTTTTATGGTGGGACGAGGATACCTGTCTCCAG ATCTCAGTAAGGTACGGAGTAACTGTCCAAAAGCCATGAAGAGATT AATGGCAGAGTGCCTCAAAAAGAAAAGAGATGAGAGACCACTCTTT CCCCAAGAGAATTTGCAGCCTTCAAGTAGCCACCATCATGGCAGCA TCTGCTCTTATTTCTTAAGTCTTGTGTTCTGACAAATTTGTTAACATCA AAACACAGTTCTGTTTCTCAAATCTTTTTTTAAAGATACAAAATTTCC AATGCATAAGCTGA</p>
hBRAf-ref 3'UTR (NM_004333.6)	<p>aacaaatgagtggagagagttcaggagagtagcaacaaaaggaaaataaatgaacatatgtttgc ttatatgttaaattgaataaaaatactctcttttttaagggtgaaccaaaagaa</p>
hBRAf-X1 3'UTR (NM_001354609.2)	<p>ccaccatcatggcagcatctgctcttatttctaagtctgtgttcgtacaatttgtaacatcaaaacaca gttctgttctcaaacttttttaagatacaaaattccaatgcataagctgatgtggaacagaatgg aattcccatccaacaaaagaggaaagaatgttttaggaaccagaattctctgctgccagtggttcttc aacaaaaataccacgagcatacaagtctgccagctccaggaagaaaaggagagaccctga attctgacctttgatggcaggcatgatggaagaaactgctgctacagctgggagatttgctatgg aaagtctgccagtcaactttgcccttcaaccaccagatcaattgtggctgatcatctgatggggcag ttcaatcacaagcatcgttcttctgttctggaatttggagcttcccctagtaccacca gtagttctgagggatggaacaaaatgcagctgccccttctatgtgtgctgttcaggccttgaca gattttatcaaaaggaaacttttattaaatggaggctgagtggtgagtagatgtgcttggtatgga ggaaaaggcatgctgcatcttcttctgacctccgggtctctggcctttgttcttctgctactgagg ggtctgtcaaccaagcaggctagatagtgctggcacacattgccttcttctcattgggtccagcaat gaagataagtggtgggttttttttctccacaatgtagcaaatctcaggaaatacagtttatcttc ctcctatgctcttccagtcaccaactacttatgggctactttgtccagggcacaatgcccgtggcag</p>

tatctaactaaacccccacaaaactgcttaataacagtttgaatgtgagaaatttagataatftaat
ataaggtacaggtttaaattctgagttctcttttctatttttatataaaagaaaataatcttcagatttaatt
gaattggaaaaaaacaatactcccaccagaattatatactctgaaaattgtatctttgtatataaaca
acttttaagaaagatcattatcctttctctacctaataatgaggagcttagcataatgacaaaatfttat
aattttcaattaatggactgtgctggatccacactaacatcttgctaataatctcattgtttctccaactg
attcctaacactatacccacatctcttctagtctttatctagaatgcaacctaaataaaaatggg
ggcgtctccattcattctcctctcctttttccaagcctggcttcaaaagggtgggcaattggcagct
gaattcccagacagagaatagagcaatttagggatattaggactgagggaggggtgggaaagc
tgcacatcagttgtttatagaaagaactggcattcattaagaacctaaatcttatcttgcacaaatgga
aaataaacctagttatagctccttggcctttataaagggttaataatcaatcacagctatagcaaaga
aagcggatgtatfaatggcaattaatggaaaacctcccttatcaggaatctagactcagaatftag
gaacacaaatcaaatcagaccaaccaagctatagccaaggactgaaagaaatfaaaacaagac
ccagaataaatcaaggaattgaaattgtatftaaaaatcttcagattgtaactccaggccctgctgtct
atattgcagccactaaaagctcactaccattagattttgctaacatacatgtattcagaagaaagcct
attgaaatctcattgtctgtaaaagggtgtcctagtaaaaatggaaaagatccttaagttatfaatcagtt
gaaaagcaaatgttttaagtttacatcagcagggcagtgcttcaaaaatcagaaattgcaaag
gtgaaataatcacgctgattgagaacatctctgtgcaataatactgcctctctgaaaagcattg
gctgtttttcttttaaatatactctagatgcttttaaatgtggctgtgtcccttaccagattggctcaa
gtttccgcaggtagagagacctgggcttgaacaagaggatgtgttcatgtctgtgaggaggtag
aacatgtgcagcctgggtccgggactgcctccgtggggcaggggcaagggcggtaccattaggg
aggaagcttagcatttcagttcttaaacatattcagggatgatacacttttctccctgcattttagaat
aggctggtatctcatttgaacgggggagcagactgtatcfaatgaagctgtgccaggagccag
gcttagcattatgagattttatagataccttaaaaaataaaatattfaaacctctctttctcctttctatg
aaataggttttctctagtttcaaatgacatgaaaataggttttattgtgtttatctgctttttttgatgc
ttagacaacagttagactactgagctcctaaaaaacgaggaagaagccttattgtgaaaagc
actttatgagtaattgtatagacagatgtggctgctgactgatcatctgtgaagggtgtaacagctctg
tctgtaaagtggtgagctgcctctgtagtggtttatgtttggtagggagagggtgaagcctctgaaa
aatgtgagagcaactacagaggattgtttgtaactgtgtatctctgatggactttttcatcgtagag
tcaaggacctagactttgacctgaaataatgacccaaaaaatagtttataaaagggtattgtg
aatagaaaatcagtgatcattgtgttaatgtgcaccttaaaagaagattctgtctagctgtcaaat
tctggtcccgaatatctcaccctgattgtatftgagatctagtagggcatactggggcattttagaag
ataaaatcccatacaaatgatatagtctatattatgttggtgttgagaagaaagagcagtatataa
agaaataattcaagactgcagcactgtcaacctgaaactttgtaaatttcttagctctggtttggg
cgggtgacagcacttcatcacaggatgttacctgtattcaccaggcggagtgcgagctgctgcacat
cctctcagatctcacctgtcccactgtacatccaccgccaagctgcttgcaaacctcatctctagct
ttagttcgaaccacattgcaggggtcaggtgacctctcaaaaaactacctctcagaatgaggta
atgaatagttatttttaaaatagaaaagtcaggagctctagaacatgacgatatttaagatttta
actttttgtgactgtatttgagcactctcattttgtcctaaagggcattatacatttaagcagtaatactgt
aaaaaaatgtgtgctcggaatatctgaatgtgttgaaagtggtgccagaaccggtttaggggtacg
ttcagaatcttaacctgagcaattgcatgaaatfaaatagctgtggtatcacttactaacagtgatg
taattftaatttcagtaggcttggcatgacagtaacatctcataatgagttgtctgcagctttgtcacatg
cacaggcattcatagaaagaccaccagctaagagggtagaatgattactcttttgcaagattctct
tctttgtcaaagttggcattgtatgtgctaggaataaccagcacctgagacgagcagattccaaccatt
aggctataaacaccatagccagagatggaagggttactgtgagatgaacagcaaatagcttaca
ggctatgagttgaaatgggttaggtgaggctctagaaaaataccttgacaattgccaatgatctta
ctgtgcctcatgatgcaataaaaaagctaacattttagcagaatcagtgattgtgaagagagca
gccactctggtttaactcagctgtgttaataatfttttagagtgcaatttagactgcataggttaaatgact
aaagagttatagccaaaatcacatttaacaatgagaaaacacacaggtaaatcttcagtgaaaca
aattatfttttaagcacataatccctagatagtcagatataatfttatcacatagagcaactaggttga
aataatagttcagtgacatttctagagaaacttttctactccataggtcttcaaagcatggaactfttat
acaacagaaatgttgacagaaattgctgtagtttaggggtgaaactgtatgtatggggcagcaatcat
gtattaacttagaaggggaaattgaaataataggaccgaatttggtttatcagttccagagactgctg
ccaacctgacactgattttcagagtttgaatgtaaatttctcccgggactgtattgcacatgaagc
tggactgctgttagtcatcctgtcccaaagcgtgtgggggcccagggtggaggctcaaggcatcctt
atgacctggccattggatgtaaaagaaaacatattccatgctgtgggtctgtatctgtttcattcctcac
cattgaaagagaaagtcattgtattgtctccagcacatccttgaatgttatactgggatggattactg

atgccatcggtagttgagccccagaagaggtagtagcatctctgcctcaggtgatgattgtagct
tggccagaggagagcggagtcaccagtatactgtgggccatgttgctagctctggtaaaattaa
atactggaagatggtgtttattagtagactagacagtaagctctgtttgtgtttcaaataacctat
cactttgtttgggcaaagacatttaaattgaaattcaattctaattttgttaattgtggaaaggtaatta
acagttcctatcaggtattttaatgtggaaaaggacagaaaccaactcctaaaatctaaattaag
gtaacagtgcttataaaaaaaaaaatgcatggggcaattagtcggcaactcaatgagtgactaaa
gtacttttatttaacatccacaactcaactgttaagttttattaattactaaatcagctttataaaatgtg
acatttatttagctattttgaataattatagtgacttgacgagtggtatgaggacacagccaatgtaag
ccagtgatccatttttagagggtcatttttttaagaattctgtagatagaagtgctctgaaaaaac
taaaatagtttattcatggtagatcaaaaaatgtttgtacaaaccatctgcttctccggccagccga
gttcattctccagcaccgtgaccgtggttctcatgtacagcacatatgcgggagagttggcagaaa
atgtggaagagatgccgcaaaggaagggtctgtgacgggtgggattgggggtttgatgaagttg
ctagtctgtttgtttgaaaataactgctgtcattttgtgttaagttttgaaccacgtgttttggtg
gagtagagttggaagtactgcaaaactagcataaaacaacaaagctcacagagtaggcacagat
gtagagaacagagaccaaaatggggtaggtggcagtaaactagtagggaaaaattaatgt
gaggggtgggaaataaactgtaattacctgaaatcaaatgtaagagtgcaataagtagcttttattct
aagctggaacgggttttaagaatcattcctcctaatacatttgtagtccatagctgattaaaacc
agctatacaacatataatgccttttattcatgttaatgaccaacgtaagtgctagccttattgtctat
atcttcatgttatgttagttacatacaggggtgtatgtctctgtgctgcccctctcctgccttca
atgcatccatgggtcctccgtgttcccttggccatgccacatatagactcagttggccttcatgat
cgctgattttgaggactgtatcacagtgatgtatgtttgtggaatctcattgttggtgtacatctgat
ctttcctcaacatggcaattgctgccttccctaagataggatcatacaactgatcaggggattgaattg
atcattcatcaacatgtgtctctgaattttattcagtagttgtcattgtccttggtttagaccaagaaaaag
gaaatcccccttttcatgtattccttggttgaggacatgactcctgtaaggagagggaaagggaga
tgcttctgtttgaactgcagtgattcacgggtcctgttccaccactcctaaacctatggcgactcacac
acacattcctctttctgttactgccaaggttcgggttagtacacttcagttccactcaagcattgaaa
agggtctctgtggagtctggggcgtgccagtgaaaagatggggacttttaattgtccacagacctct
ctatacctgcttgcataaaatacaatggagtaacttttaagctattttcaattcataaaaaaga
catttatttcagcaaatggatgatgtctcctctttccctattctcaatgtttgcttgaatctttattttt
tttaattctccccatacccactcctgatactttgttctcttctgctcagggtcccttattgtactttgga
gttttctcatgtaattgtataacagaaaaatattgttcagtttgatagaagcatggagaataaaaa
aagatagctgaaattcagattgaagaaattttattctgtgtaaagttatataaaaactgtattataaaaa
ggcaaaaaaagttctatgtacttgatgtgaatagcgaatactgctaataaagattgactgcatgg
agaa

Supplementary Table 1. Primer sequence and use.

Primer	Sequence 5' → 3'	Use
hBRAFcds common-Sall-Kozak sequence -Fw	ATAGTCGACGCCACCATGGCGGCGCTGAGCGGT	hBRAFcds cloning
hBRAFcds ref cds Spel stop codon Rev	ATAACTAGTTCAGTGGACAGGAAACG	hBRAFcds ref cds cloning
hBRAFcds ref X1 Spel stop codon Rev	ATAACTAGTCTACTTGAAGGCTGCAAATTCTC	hBRAFcds-X1 cds cloning
hBRAFcds ref X2 Spel stop codon Rev	ATAACTAGTTCAGCTTATGCATTGGAAATT	hBRAFcds-X2 cds cloning
hBRAFcds ref 3'UTR Spel Fw	ATAACTAGTTGAAACAAATGAGTGAGAGAG	hBRAFcds ref 3'UTR cloning
hBRAFcds ref 3'UTR NotI Rev	ATAGCGGCCGCTTCTTTGGTTCACCTTAA	
hBRAFcds-X1 3'UTR Spel Fw	ATAACTAGTTAGCCACCATCATGGCAGCATC	hBRAFcds-X1 3'UTR cloning
hBRAFcds-X1 3'UTR NotI Rev	ATAGCGGCCGCTTCTCCATGCAGTCAATCT	
hBRAFcds_377 Fw	CTAGCCTTTCAGTGCTACCTTCATCT	common cds RT-PCR
hBRAFcds_1001_Rev	GGACTGGTGAGAATTTGGGGC	
Ex14_1705 Fw	GCCAAGTCAATCATCCACAG	ref cds specific RT-PCR
hBRAFcdsRef_2300_Rev	CAGTGGACAGGAAACGCACCATAT	
Ex15_1841 Fw	CTGGATCCATTTTGTGGATG	X1/X2 cds specific (ex19) RT-PCR
hBRAFcdsX1_2300_Rev	CTTGAAGGCTGCAAATTCT	
Ex17_2075 Fw	TAATGGCAGAGTGCCTCAA	ref cds-3'UTR junction specific RT-PCR
hBRAFcdsFutrRef_38 Rev	TGTTGCTACTCTCCTGAACTC	
X1 only qRT_2179 Fw	AGTGCATCAGAACCCTCCTT	X1 cds-3'UTR junction specific RT-PCR
hBRAFcdsFutrX1_387 Rev	TTGATCTGGTGGTTAGAAGGG	
hBRAFcdsFutrX1_6041Fw	TGTTAATGACCAACGTAAGTGGC	X1 3'UTR end specific RT-PCR
hBRAFcdsFutrX1_7155 Rev	GCAGTCAATCTTTATTATAGCAG	
actb1_Intr311_Fw	TCAGGGAGTGATGGTTGGC	RNA control, exon spanning RT-PCR
actb1_Rev	CAACGGAAACGCTCATTGC	
eef1a1l1_Fw	GTA CT TCTCAGGCTGACTGTG	Housekeeping qRT-PCR
eef1a1l1_Rev	ACGATCAGCTGTTTCACTCC	
actb1_Fw	TGAGCAGGAGATGGGAACC	Housekeeping qRT-PCR
actb1_Rev	CAACGGAAACGCTCATTGC	
hBRAFcds_377 Fw	CTAGCCTTTCAGTGCTACCTTCATCT	Hsa specific/common coding BRAF qRT-PCR
hBRAFcds-qRT1 Rev	TCCGTGCCACATCTGTGGGAT	